

Repowering Chinese coastal ferries with battery-electric technology: Operational profiles of Chinese coastal ferries, their energy demand, and the implied battery system assessment

Authors: Xiaoli Mao, Elise Georgeff, Dan Rutherford, and Liudmila Osipova

Keywords: battery-electric, zero emission vessels, ferries, voyage pattern, GHGs

Introduction and background

The International Maritime Organization (IMO) fourth greenhouse gas (GHG) study shows a growing impact from domestic shipping activities (Faber et al., 2020). The study found that up to 30% of global shipping emissions are associated with domestic shipping, highlighting the potential for more state-level actions. In November 2020, the IMO's Marine Environment Protection Committee adopted Resolution MEPC.327(75), which encourages countries to develop and submit voluntary national action plans detailing how they intend to address GHG emissions from ships. China is one of the original sponsors of the proposal to develop national action plans. In June 2020, the Chinese Ministry of Transport (MOT) announced its strategic development guidelines and 2050 targets for inland waterway transportation, in which clean energy will be used in vessels, including batteries and fuel cells (MOT, 2020b).

Initial applications of zero-emission technologies in the maritime sector have targeted smaller-sized applications with short, fixed routes. As shown in Hall, Pavlenko, and Lutsey (2018), passenger ferries have seen the most progress toward electrification, and several battery-electric ferries are already on the water, mostly in Europe. Denmark's electric ferry (e-ferry) *Ellen*, in service since 2019, carries by far the world's largest battery system of 4.3 megawatt hours (MWh) which can power a one-way route of 22 nautical miles. It uses an onshore charging station with a charging power as

www.theicct.org

communications@theicct.org

[twitter @theicct](https://twitter.com/theicct)

Acknowledgments: This work is generously supported by the Heising Simons Foundation. The authors thank Dr. Bryan Comer and Amy Smorodin for their critical review of this paper, exactEarth for providing Automatic Identification System data, and IHS Fairplay for providing ship characteristics data. The authors also thank Dr. Anita Graser, who created the *MovingPandas* Python package and generously made it open access.

high as 4 MW.¹ More importantly, the *Ellen* design is scalable in terms of size, capacity, power, and speed to service most regional ferry routes in Europe (Kristensen, Nielsen, & Heinemann, 2018).

The use of a similar e-ferry prototype in China could also help to speed up the market uptake of electric ferries and to begin domestic ship decarbonization in the country. In 2019, 273 million passengers were moved by ferries in China (MOT, 2020a), nearly triple the passenger throughput of Hartsfield-Jackson Atlanta Airport, the world's busiest airport in the same year (Graver, Rutherford, & Zheng, 2020). Battery-electric ferries offer an opportunity to transform China's ferry industry by offering an energy-efficient, and less polluting mode of passenger transportation. In June 2020, China's first battery-electric passenger ferry, *Jun Lv Hao*, took its maiden voyage on the Yangtze River (Cao & Ye, 2020). China is debuting another battery-electric cruise ferry in late 2021, reportedly the world's largest, with a battery system of 7 MWh ("Chinese all-electric river cruise vessel," 2021).

In order to understand the market potential of electrifying Chinese coastal ferry fleet, we need to understand the current fleet composition and operational profiles, which are crucial to determining applicable technologies for vessels and associated shoreside infrastructure. Few studies have systematically analyzed ferry operations in China, although there are some studies that focus on ferry service network design in Hong Kong (An & Lo, 2014; Andersen, Crainic, & Christiansen, 2009; Chu, Shao, Xu, & Kang, 2020; Lai & Lo, 2004; Wang & Lo, 2008). An overview of urban waterborne transport system by Cheemakurthy and colleagues (2018) provided a snapshot of ferry operations in Hong Kong, with ferry and terminal features (passenger capacity, terminal facilities, etc.), operational characteristics (schedule, frequency, fare, etc.), and a map with color-coded major ferry lines; but the information was high level. With the addition of ship movement data, detailed ferry operations can be analyzed using ICCT's Systematic Assessment of Vessel Emissions (SAVE) model as described in Olmer, Comer, Roy, Mao, and Rutherford (2017).

In this study, we use the SAVE model to analyze real-world coastal ferry movement data in February of 2019 in China, identify and characterize voyages, and evaluate the feasibility of repowering the coastal ferry fleet with battery-electric technology.

We found that existing battery technologies already can satisfy most application scenarios for China's coastal fleet, namely smaller ferries deployed on shorter routes, which could be the first movers of battery-electric ship uptake. Battery technology improvements in the near future are key to boosting the battery-electric ship uptake in the "harder-to-electrify" segment of the Chinese coastal ferries, which consists primarily of larger ferries deployed on longer routes. With improved battery technology, we found that for passenger ferries, targeting ships up to 55 meters (m) in length and routes up to 100 kilometers (km) would replace 50% of fossil fuel use with electricity; for passenger-and-car ferries (ro-pax), the same fossil fuel replacement target can be attained by targeting ships up to 170 m in length and routes up to 200 km. Among the more than 16,000 ferry operations completed by 129 passenger ferries and 80 ro-pax ferries in February 2019, more than two-thirds of operations took place in the Pearl River Delta region. Electrifying all coastal ferry operations in the Pearl River Delta region could eliminate more than 30% of the fossil fuel used by the entire Chinese coastal ferry fleet

¹ Information about e-ferry *Ellen* can be found on its official website, <http://e-ferryproject.eu/>

in February 2019. Electrifying ferry operations in the Bo Sea region and the Hainan Strait could enable an additional fossil fuel replacement of more than 40%.

Methods

The SAVE model is primarily used for generating high-resolution spatiotemporal ship emission inventories (Olmer et al., 2017). With this paper, we introduce a new function of the SAVE model—route identification. This study, which is part of our zero-emission vessel (ZEV) research series,² evaluates the feasibility of electrifying the Chinese coastal ferry fleet.

In the following subsections, we explain how we evaluated the feasibility of powering ferries with batteries and how we calculated the share of fossil fuel consumption that could be replaced with electricity.

Route identification

In this analysis, we use *operation* as a general term to describe ferry movements between origin and destination. We also define three terms, *leg*, *voyage*, and *route*, as follows:

- » Leg: Any continuous ferry movement between two full-stop points. Full-stop means the ferry shuts down its propulsion engine and a point is usually a terminal at a port.
- » Voyage: A journey between origin and destination. A voyage may consist of one or more legs.
- » Route: The pathway between an origin-destination pair. Ferries sail repeated voyages along routes.

Each ferry serves one or multiple routes. On each route, a ferry traverses a certain number of voyages within a given time. Each voyage can comprise one or multiple legs (see Figure 1).

In this analysis, we focus on operations of Chinese coastal ferries³ made in February 2019,⁴ identified from their Automatic Identification System (AIS) data. As indicated in Olmer et al. (2017), ferry operations differ from those of cargo ships in that ferries have much shorter time resting in ports (or terminals) between two consecutive legs. Detailed ferry route information provided in Leung et al. (2017) shows that the one-way trip time of key Hong Kong ferry routes is less than 60 minutes. As a result, the AIS data are first aggregated to the minute and we linearly interpolate location and speed for missing minutes. This is a departure from the way SAVE is typically used. In previous work, we aggregated and interpolated by the hour; however, if we followed that process in this analysis, we would miss large portions of voyages given the relatively short distances coastal ferries travel along their routes. With minute-level aggregation and interpolation, if a ship was observed in the AIS data beginning at 00:00 and ending at 23:59, we will have a total of 1440 records that day including observed and interpolated records. These data are the main input of the route identification function.

Our route identification function is enabled by a Python package called *MovingPandas*, a geospatial analysis tool for extracting trajectories from movement data (Graser, 2019).

² Other publications in this series include Mao et al. (2020) and Georgeff, Mao, Rutherford, and Osipova (2020).

³ Ferries registered with a valid IMO number and flagged to P.R. China or Hong Kong S.A.R.

⁴ February marked the peak ferry traffic month in 2019, due to traffic surge associated with the Chinese Spring Festival.

A trajectory is a vector, defined by timestamps, direction, and speed. In our application, we use *MovingPandas* to create one trajectory for each individual ship wherein all its AIS points are joined; each trajectory is then analyzed to determine if there is an interruption, such as an observation gap or an anomaly in speed. These interruptions are times when ships are at berth at a terminal in a port. The SAVE model has a function to identify whether a ship is at berth based on its speed and its proximity to a port based on a database of ports from World Port Index (National Geospatial-Intelligence Agency, 2019). For this project, we enhance this function by adding ferry terminals using a database made available by Open Street Map.⁵ This allows us to create “observation gaps” by removing AIS signals associated with at-berth activities. The split segments of a trajectory, or individual legs of a voyage, are assigned unique identifications. A summary diagram of the route identification function is shown in Figure 1. In the diagram, a ship traveling from port A to port C has completed one voyage consisting of two legs, and the ship is sailing along the A-C route.

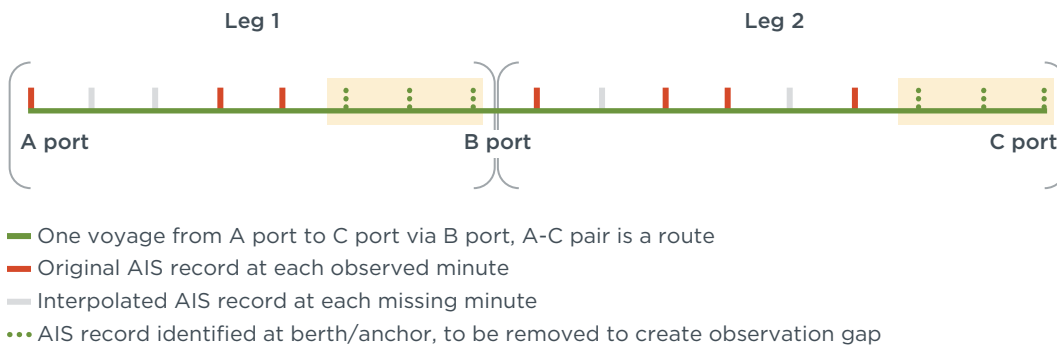


Figure 1. Route identification procedure.

Feasibility assessment for ferry electrification

Feasibility for a leg and for a ship

Similar to the method used in Mao, Rutherford, Osipova, and Comer (2020), the feasibility for a battery-electric coastal ferry fleet in China is first evaluated at the leg level. Using the SAVE model, we estimated the amount of energy required for each identified leg. This energy was converted to the equivalent volume and mass of a battery system using the following equations similar to those used in Mao et al. (2020) but with the updated assumptions listed in Table 1.

Equation 1

$$BV_l = \frac{RE_l}{BD_v \times \eta \times DoD}$$

Equation 2

$$BM_l = \frac{RE_l}{BD_m \times \eta \times DoD}$$

Where:

BV_l = Volume of the battery system to provide the energy required for leg l , in m^3

RE_l = Required energy for leg l , in kWh

⁵ © OpenStreetMap contributors. Data are available under the Open Database License found at <https://www.openstreetmap.org/copyright>

BD_v = Volumetric density, or energy density of battery system,⁶ in kWh/m³

η = Battery efficiency

$DoD = 0.75$, which is our default assumption on depth of discharge, or the percentage of the battery-stored energy that the ship can use without damaging the battery

BM_l = Mass of the battery system to provide the energy required for leg l , in tonnes

BD_m = Gravimetric density, or specific energy of battery system,⁷ in kWh/tonne

In Minnehan and Pratt (2017), the authors collected specifications for battery systems that had been used in marine applications at that time, which averaged 72 kWh/m³ for energy density and 75 kWh/tonne for specific energy (right most column in Table 1). Those assumptions represent current battery technology, which is constantly evolving. According to ICCT's recent work (Slowik, Lutsey, and Hsu, 2020), anode improvements could increase gravimetric density at the battery cell level by 15%, and cell-to-pack level improvements could increase pack-level gravimetric density by another 20% by 2030 for a given battery chemistry. Because we are evaluating the full potential of electrifying the Chinese coastal ferry fleet, we include “near future” assumptions on battery energy density based on the BatPac model (Argonne National Laboratory, 2020).

Table 1. Key assumptions on battery system specifications for ferries

Inputs	Near future	Current
Energy density (kWh/m ³)	370	72
Specific energy (kWh/tonne)	200	75
Battery efficiency	90% ^a	
Depth of discharge	0.75 ^a	

Note: ^aThese assumptions are consistent with those used in Comer (2019).

The volume and mass of the needed battery system are compared with the available volume (AV_{max}) and mass (AM_{max}) a ferry can accommodate without changing its design, which is calculated in the same way as described in Mao et al. (2020) and Comer (2019). A leg is considered “attained” only if both the battery volume and the battery mass needed to accomplish a leg are less than the volume and mass available for the ferry. If all the legs constituting a voyage are attained, the voyage is considered an attained voyage. Finally, if all legs made by a ship are attained, the ship is considered an attained ship. The leg attainment rate (LAR) is calculated as the total number of attained legs divided by the total number of legs, whereas the ship attainment rate (SAR) is calculated as the total number of attained ships divided by the total number of ships. A ship's battery range, the maximum distance a ship can travel without having to recharge, can also be used to evaluate a ship's electrification potential. Similar to the method used in Mao et al. (2020), we calculated each ship's battery range assuming 75% maximum continuous rating operations as typical.

Feasibility re-evaluated with charging constraints

Refueling constraints were not considered in Mao et al. (2020), which investigated the feasibility of replacing fossil fuels with liquid hydrogen fuel cells for container ships along the transpacific corridor, because container ships usually berth long enough to

6 Please note that the unit of Wh/L is equivalent to the unit kWh/m³. Although we use kWh/m³ in this analysis, much of the battery-related literature uses Wh/L instead.

7 Please note that the unit of Wh/kg is equivalent to the unit kWh/tonne. Although we use kWh/tonne in this analysis, much of the battery-related literature uses kWh/tonne instead.

sufficiently refuel. However, ferries usually have shorter berthing times and battery recharging is expected to require more time than hydrogen bunkering. The amount of battery energy recharged between two consecutive legs is determined by charging power and charging time. In this analysis, we conserve all existing ferry operation patterns, meaning the charging constraint comes only from charging power, measured in kW or MW. In the previous section, we explain how LAR and SAR are calculated without charging constraint (green block in Figure 2). Without such constraint, each leg starts with a fully charged battery. We consider the impact of charging constraint by assuming different charging power scenarios, namely 1 MW, 5 MW, and 10 MW. With such constraints, a leg might not start with a fully charged battery (red block in Figure 2). As a result, a previously attained leg could become unattained (leg 2 in red block in Figure 2). This added constraint would reduce the overall feasibility of ferry electrification.

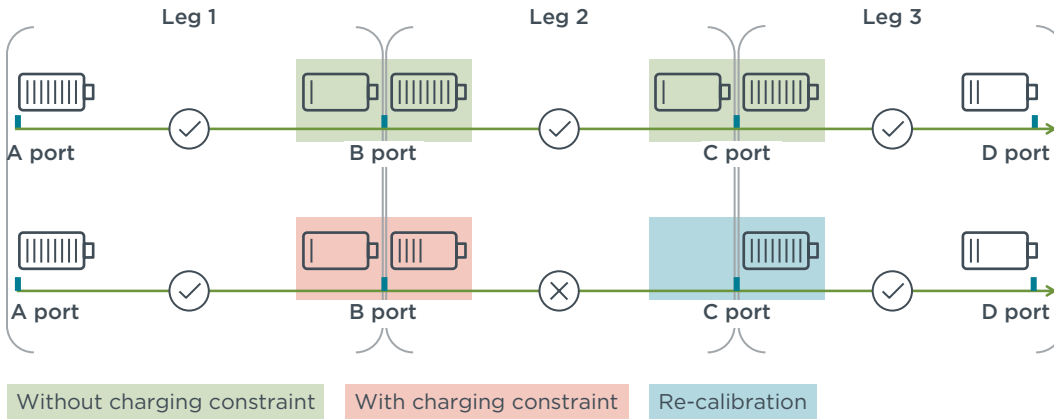


Figure 2. Flowchart of incorporating charging constraint into feasibility evaluation.

We label a leg as attained only if the amount of battery energy available at the beginning of the leg (AE_j) is greater than the energy required for the leg (RE_j). The amount of battery energy available at the beginning of a leg is determined by the battery energy remaining from the previous leg plus the amount of battery energy recharged during berthing between the two legs, as shown in Equation 3. We perform this iterative calculation chronologically for each ship and assume the battery is fully charged at the beginning of a ship's first leg, the power of which is determined by the available volume (AV_{max}) or mass (AM_{max}) a ferry can accommodate without changing its design. This is shown in Equation 4. Once a leg is labeled as unattained, the beginning battery energy available for the next leg is recalibrated to a fully charged battery (blue block in Figure 2).

Equation 3

$$AE_{j+1} = AE_j - RE_j + CP \times T_j$$

Equation 4

$$AE_j = \min(AV_{max} \times BD_v, AM_{max} \times BD_m)$$

Where:

AE_{j+1} = Available battery energy onboard a ship before the ship starts leg $j+1$, in kWh

CP = Charging power, in kW

T_j = Available amount of time for charging after leg j before the ship continues to leg $j+1$, in hours

Once each leg is determined to be either attained or unattained, the LAR and SAR are recalculated in the same way described in the previous section.

Calculating the share of fossil fuel potentially replaced by battery electrification

Like the energy required for each leg, the associated fossil fuel consumption can be calculated directly using the SAVE model. The amount of fossil fuel associated with legs and ships that are identified as attained in the previous step is considered to be potentially replaced with electricity if these legs and ships were to be powered by battery. As a result, the share of fossil fuel potentially replaced with electricity can be calculated and summarized at different levels.

The results are discussed in the next section. First, we present the results based on the near-future battery specification assumptions; we then conduct a sensitivity analysis based on current battery technology.

Results

Characteristics of the existing Chinese coastal ferry fleet

The makeup of the Chinese coastal ferry fleet of February 2019 was found to be 209 ferries, including 129 passenger ferries and 80 ro-pax ferries. These ships have a range of passenger capacity, with smaller passenger ferries capable of carrying about 200 people and larger ro-pax ferries capable of carrying more than 1,500 people plus about 150 cars. Table 2 provides a detailed summary of the characteristics of these ferries.

Table 2. Characteristics of the Chinese coastal ferry fleet, with estimated battery range and capacity

Ship class	Size category ^b	Average ship length (m)	Number of ships	Average passenger capacity per ship	Average vehicle capacity per ship	Average main engine power per ship (kW)	Average max speed per ship (knots)	Average battery range per ship (km) ^c	Average battery capacity per ship (MWh) ^d
Passenger ferry ^a	1	31	28	191	NA	3,568	34	1,110	55.8
	2	43	94	277		5,310	35	884	60.2
	3	65	7	264		3,078	18	391	47.6
Ro-pax ferry	2	70	15	514	29	3,763	18	337	40.2
	3	110	12	802	40	5,494	15	386	66.0
	4	134	34	1,041	79	6,482	15	472	95.6
	5	174	19	1,530	149	12,840	18	287	154

Notes: ^aMost passenger ferries are now high speed, although some older large cruise ships are repurposed for ferries and travel much slower than the newer ferries. ^bThe size category is based on the ship's gross tonnage. This categorization is consistent with Faber et al. (2020). ^cBattery range is not directly linked to attainability of operations; the charging constraint, the route length, as well as scheduling flexibility all play a role, which we discuss in the later sections. ^dThe capacity values calculated with available volume and available weight are different. We present the values based on available weight, which is the smaller set of values.

In February 2019, passenger ferries consumed 5,036 tonnes of marine diesel oil (MDO) and 79 tonnes of heavy fuel oil (HFO) whereas ro-pax ferries consumed 1,244 tonnes of MDO and 8,407 tonnes of HFO. The average installed main engine power of passenger and ro-pax ferries was around 4,497 kW and 7,226 kW, respectively. Ro-pax ferries are generally larger in size, carry more passengers, and can carry vehicles but they travel much more slowly than passenger ferries. The battery range values of these ships vary significantly. On a single charge, most ro-pax ferries cannot travel farther than 500 km, whereas most passenger ferries could potentially double that range.

Figure 3 maps all the Chinese coastal ferry traffic in February 2019 and visualizes traffic density. By zooming in on five key coastal economic zones along the coast, one can clearly observe the differences in use of ferries. In the Bo Sea (A), Taiwan Strait (C), and Hainan Strait (E), ferries are used in lieu of a fixed link, such as a bridge or tunnel, between two destinations; for the Yangtze River (B) and Pearl River Delta (D), ferries are used to connect the many outlying island communities to the mainland.

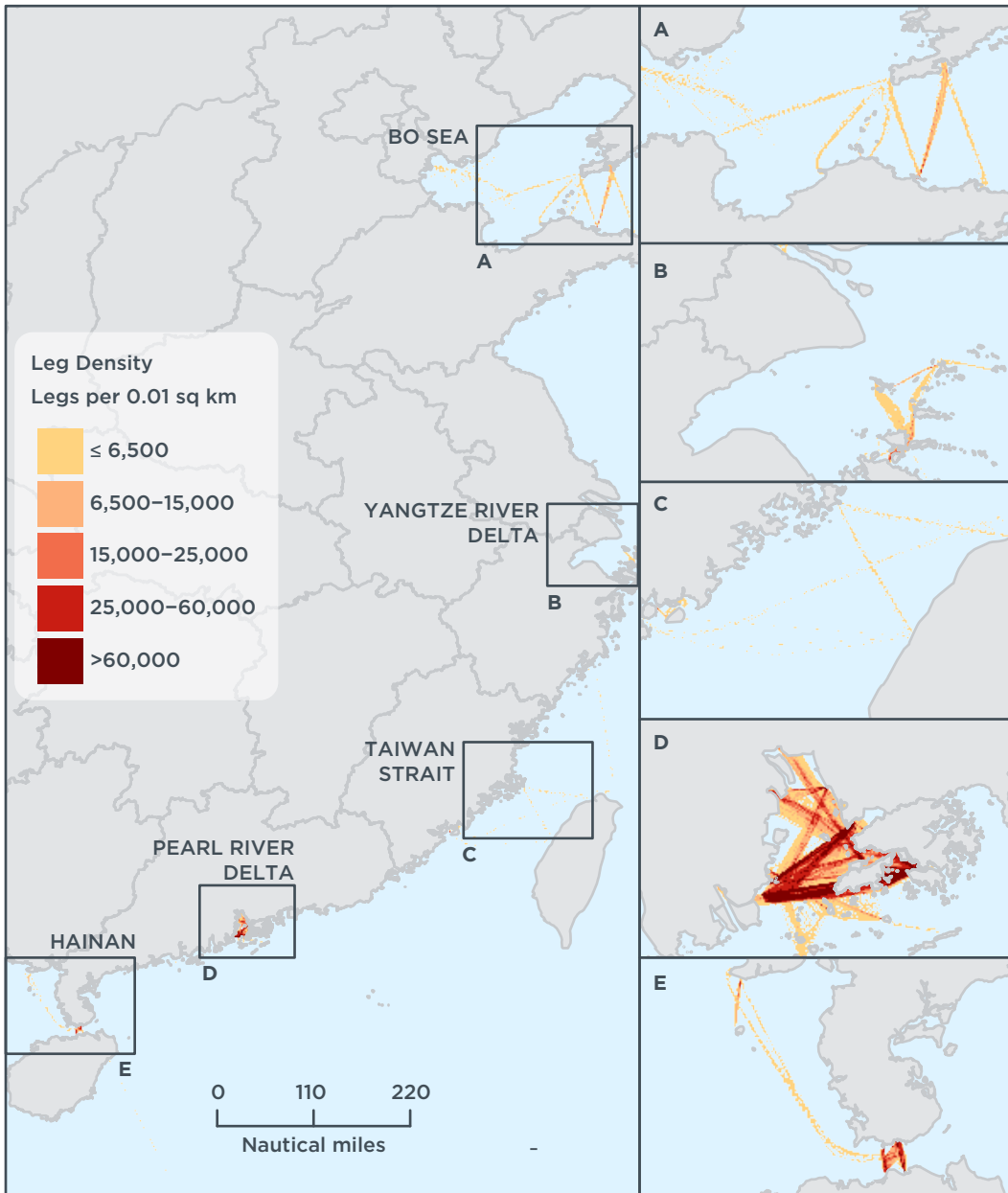


Figure 3. Chinese coastal ferry leg density in February 2019.

We identified more than 16,000 individual legs belonging to approximately 208 routes characterized by distinct origin and destination pairs for ferries plying China’s coastal waters in February 2019, scattered across the five major coastal economic zones identified in Figure 3. The Pearl River Delta (region D in Figure 3), home to major cities like Guangzhou, Shenzhen, and Hong Kong, saw two-thirds of the total ferry traffic

analyzed in this study. In Table 3, we selected two sample routes per region and present summary statistics along these routes for February 2019.

Table 3. Characteristics for selected routes in China’s coastal waters in February 2019

Region	Route characteristics							
	Route name	One-way distance (km)	Number of ships	Number of voyages in February	Ship class	Avg cruise speed (knots)	Avg travel time per voyage (hours)	Avg energy demand per voyage (MWh)
A	Dalian ↔ Yantai	167	15	562	Ro-pax ferry	13	7	40
	Lvshun ↔ Dongying	205	1	5		10	11	43
B	Yangshan ↔ Shengsi	32	1	4	Passenger ferry	20	0.9	1
			2	93	Ro-pax ferry	10	1.7	4
	Sanjiang ↔ Daishan	15	1	13	Passenger ferry	5.5	1.5	0.8
			5	238	Ro-pax ferry	5	1.6	2
C	Xiamen ↔ Jinmen	17	2	170	Passenger ferry	12	0.8	0.3
	Xiamen ↔ Taizhong	265	1	4	Ro-pax ferry	8	18	64
D	Macao ↔ Hong Kong	63	46	1,144	Passenger ferry	23	1.5	2.7
	Guangzhou ↔ Hong Kong	85	2	12		25	1.8	2.4
E	Zhanjiang ↔ Haikou	28	29	1,223	Ro-pax ferry	7	2	3.4
	Beihai ↔ Haikou	216	1	17		8	14	34.5

Ro-pax ferries dominated ferry traffic in the Bo Sea region (A) and Hainan region (E) whereas passenger ferries were predominant in the Pearl River Delta region (D). Passenger ferries, the majority of which are high speed, sailed faster than ro-pax ferries and were more often deployed on shorter routes. The energy demand of the above 10 sample routes ranged from less than 1 MWh to more than 60 MWh. As a point of comparison, the most capable e-ferry on the water today, the *Ellen*, has a battery system of 4.3 MWh.

We also found that ferry operations, especially in high-traffic regions like the Pearl River Delta, are flexible. A ferry is often deployed on different routes to optimize ferry deployment, although this is beyond the scope of this study. Numerous research papers (Lai & Lo, 2004; Wang & Lo, 2008; Andersen et al., 2009; An & Lo, 2014; Chu et al., 2020) discuss this phenomenon specifically around Hong Kong, which means it is reasonable to assume that ferries are not restricted to one route or one schedule. Flexible ferry deployment may be common in China’s coastal waters, but there are instances where one or two ferries are dedicated solely to a route (e.g., the Beihai-Haikou route in Table 3) that is long and traveled less frequently. In the next section, we discuss the feasibility of ferry electrification based on LAR and SAR. LAR results offer insights into the feasibility of the electrification of the entire fleet if the deployment can be flexible. SAR results offer insights into the feasibility of electrification if the deployment were to be fixed and rigid.

Feasibility of electrifying the Chinese coastal ferry fleet

We find that it is feasible to electrify most legs undertaken by the coastal ferry fleet, with or without charging constraints. As shown in Table 4, we found that at the leg level, all but the largest ro-pax ferries have a LAR greater than 90% at a charging power of 1 MW. Increasing charging power to 5 MW would increase LAR across all ferries, but mildly. Without charging constraints, which means that ships are all fully charged before attempting a leg, most ships show a close to 100% LAR, even for the largest ro-pax ferries.

Table 4. Leg attainment rate (LAR) of Chinese coastal ferry operations in February 2019, if powered by batteries.

Ship class	Size category	Average ship length (m)	Number of legs	LAR under different charging constraint assumptions		
				1 MW	5 MW	No constraint
Passenger ferry	1	31	2,914	98.0%	99.7%	99.8%
	2	43	8,114	97.3%	99.4%	99.8%
	3	65	449	94.9%	96.6%	100.0%
Ro-pax ferry	2	70	846	94.7%	96.8%	99.1%
	3	110	698	98.0%	99.7%	100.0%
	4	134	2,079	92.4%	96.8%	100.0%
	5	174	935	76.3%	79.2%	96.8%

Although the impact of charging constraints on LAR is clearly demonstrated in Table 4, the impact of ship size is more subtle. For passenger ferries, LAR decreases as ship size increases when the leg is undertaken without a full battery charge. Without such constraints, LAR for passenger ferries approaches 100% regardless of size. For ro-pax ferries however, as ship size increases, LAR first increases and then decreases. For the largest ro-pax ferries, the drop in LAR due to charging constraints is significant, from over 90% to below 80%.

Even though the LAR for coastal ferries shows overwhelmingly positive results, the SAR presents a mixed picture. Without charging constraints, it is feasible to electrify most ferries and have them complete their existing operations. Except for the largest ro-pax ferries, more than 90% of all other 2019 ferry traffic studied could be fully electrified. Nevertheless, the SAR of the largest ro-pax ferries is still impressive, at about 74%. The impact of charging constraints on SAR is far more significant than on LAR. Shown in Table 5, when constrained with 1 MW charging power, SAR drops significantly, with less than half of the ro-pax ferries (5.3%–40%) and a slightly higher share of passenger ferries (42.9%–57.1%) being able to fully electrify February 2019 operations. Increasing charging power gradually, but significantly, increases the SAR, with the exceptions of the largest passenger and ro-pax ferries. Those ships need a significant boost in charging power, or prolonged time for charging, to be able to make all their operations powered by batteries.

Table 5. Ship attainment rate (SAR) of China's coastal fleet in February 2019, if powered by batteries

Ship class	Size category	Average ship length (m)	Number of ships	SAR under different charging constraint assumptions				
				1 MW	2 MW	5 MW	10 MW	No constraint
Passenger ferry	1	31	28	57.1%	71.4%	96.4%	96.4%	96.4%
	2	43	94	53.2%	71.3%	88.3%	96.8%	97.9%
	3	65	7	42.9%	42.9%	42.9%	71.4%	100.0%
Ro-pax ferry	2	70	15	40.0%	73.3%	73.3%	80.0%	93.3%
	3	110	12	41.7%	83.3%	91.7%	100.0%	100.0%
	4	134	34	11.8%	44.1%	67.6%	73.5%	97.1%
	5	174	19	5.3%	5.3%	10.5%	10.5%	73.7%

The SAR results are more useful in situations where a ship is solely deployed to service a particular route, in which case all the ship's legs need to be electrified to make electrifying the ship a reasonable choice. However, in our study, we found a complex system of ferry networks, especially in the Pearl River Delta region. Ferries operating in this region can be deployed on more than one route and multiple ships are deployed on the same route. In that case, the LAR are more useful because ferry operators can coordinate their fleet to ensure service can be maintained with an electrified fleet. Going forward, we focus on feasibility evaluated at the leg level as a result.

So far, we have discussed LAR and SAR results without considering the characteristics of each route. Without charging constraints, leg distance is the most important factor in determining LAR because running on batteries reduces a ship's range compared to fossil fuel, which can limit a ship's ability to fulfill some of its original services. The impact of leg length on LAR is shown in Figure 4.

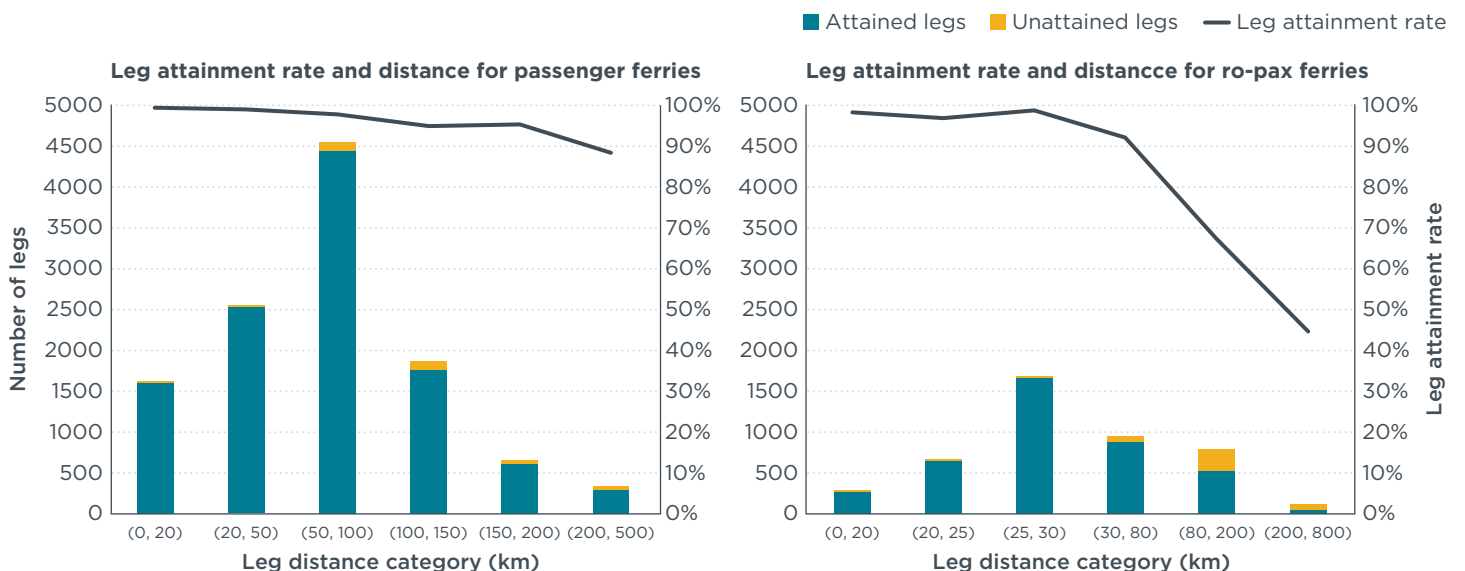


Figure 4. Leg counts and leg attainment rates of passenger ferries (left) and ro-pax ferries (right) broken down by leg length.

Both passenger ferries and ro-pax ferries show a decline in leg attainment rate as the legs become longer. Most passenger ferries traversed legs between 50 km and 100 km

in February 2019, whereas most ro-pax ferries traveled legs between 25 km and 30 km over the same period. That said, passenger ferries seldom travel more than 150 km whereas ro-pax ferries seldom travel less than 25 km. The LAR for passenger ferries is greater than 88% across all leg distances, but LAR for ro-pax ferries drops from nearly 100% on shorter legs to 50% on longer legs. Ro-pax ferries traversing legs longer than 80 km have LAR less than 70%, which falls to less than 43% for legs longer than 200 km.

Fossil fuel potentially replaced with electricity

Although coastal ferries operate along the entire Chinese coastline, they are concentrated in the five economic zones identified in Figure 3. Figure 5 shows the composition of fossil fuel burned by ferry operations per region and the respective share of fossil fuel that could potentially be replaced with electricity.

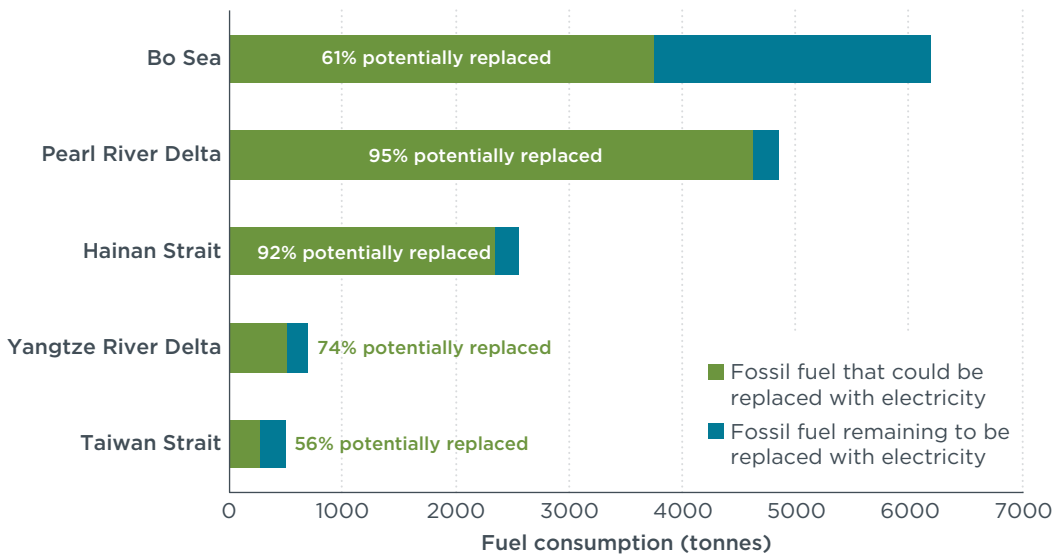


Figure 5. Percentage of fossil fuel potentially replaced with electricity by key coastal economic zone.

Among those regions, the Pearl River Delta and Hainan Strait show the greatest potential for replacing fossil fuel with electricity. These two regions account for half of the energy used by the Chinese coastal ferry fleet: 33% in the Pearl River Delta and 17% in the Hainan Strait. We found that 95% of ferry fossil fuel consumption in the Pearl River Delta and 92% in the Hainan Strait could be replaced with electricity. As previously discussed, passenger ferries predominated the Pearl River Delta region, which is the group of ships we identified as having higher LARs (see Table 4). Although larger ro-pax ferries were deployed in the Hainan Strait, the legs are relatively short, so barriers to electrifying these ships are low. On the other hand, ro-pax ferries similar in size to those deployed in the Hainan Strait were also deployed in the Bo Sea region, which saw a lower potential for electrification because legs in the Bo Sea region are longer than in the Hainan Strait. That said, the absolute amount of fossil fuel potentially replaced by electricity in the Bo Sea region is greater than in the Hainan Strait: 3,757 tonnes in the Bo Sea region compared with 2,342 tonnes in the Hainan Strait.

These results are based on near-future battery technology assumptions, as noted in Table 1. To understand the impact of battery technology improvement on the feasibility of replacing fossil fuel consumption with electricity for the China coastal ferry fleet, we recalculate LAR based on the current battery technology (see Table 1). As shown in Figure 6, battery technology today could potentially replace nearly 90% of fossil

fuel currently burned by passenger ferries. Improved battery technology, based on near-future battery technology assumptions, helps move the fossil fuel replacement percentage closer to 100%, but only marginally as illustrated by the dark red wedge in Figure 6. Improvements in battery technology have a greater impact on ro-pax ferries. As shown in Figure 7, current battery technology could potentially replace close to 50% of the fossil fuel burned by ro-pax ferries studied with electricity. The near-future battery technology could help increase the fossil fuel replacement percentage to nearly 70% as shown by the dark red wedge in Figure 7. But the improvement is negligible for smaller ro-pax ferries deployed on shorter legs. It is most helpful to electrify larger ferries deployed on longer legs, or the harder-to-electrify segment, especially for ro-pax ferries longer than 170 m deployed on legs longer than 200 km.

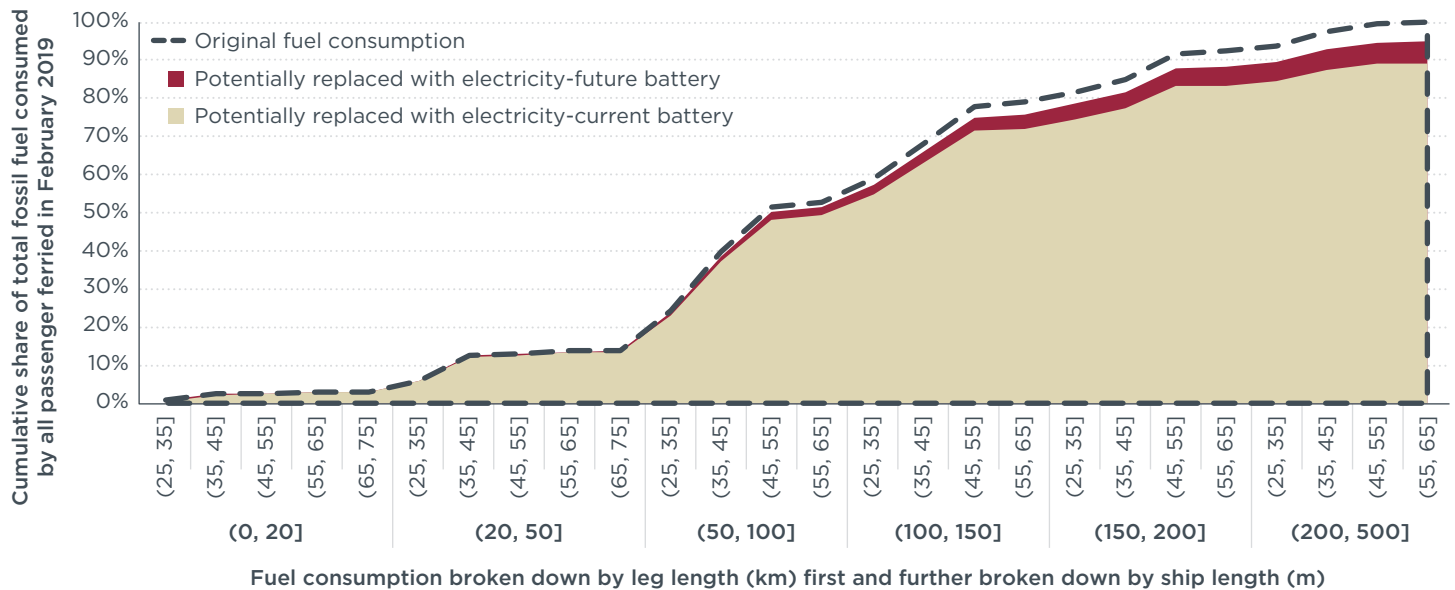


Figure 6. Cumulative percentage of fossil fuel consumption potentially replaced with electricity with current and near-future battery assumptions for passenger ferries, by ship length and leg distance, February 2019.

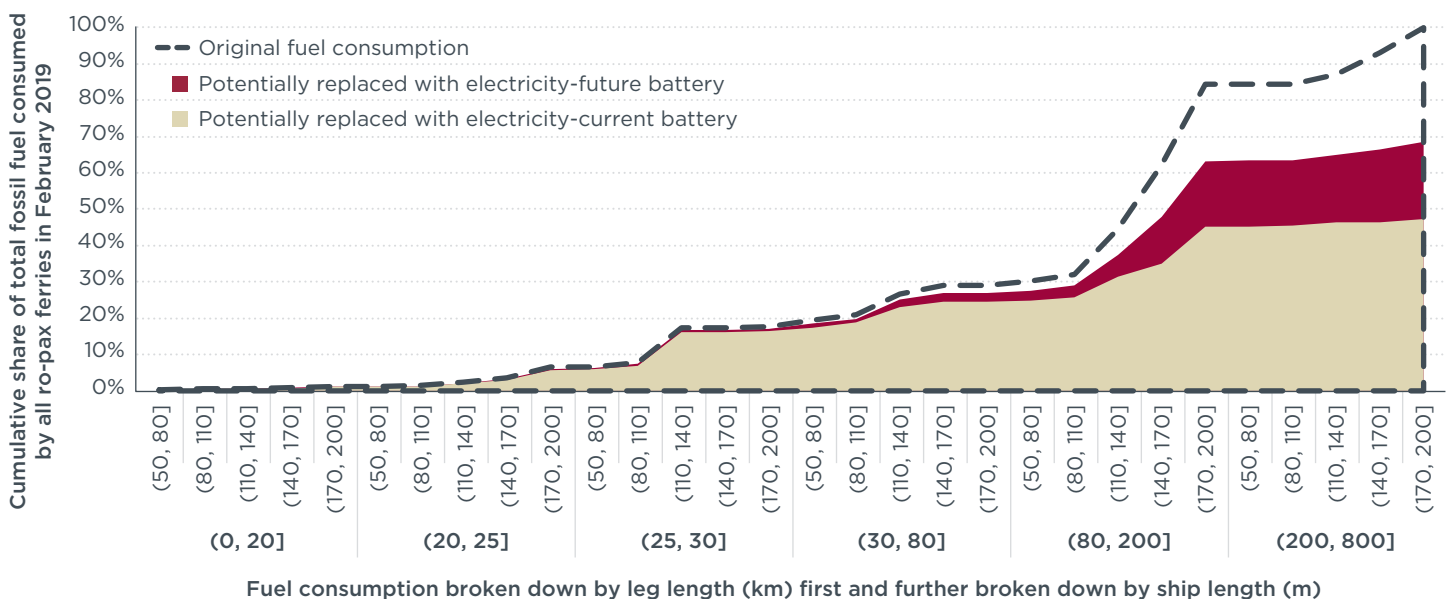


Figure 7. Cumulative percentage of fossil fuel consumption potentially replaced with electricity with current and near-future battery assumptions for ro-pax ferries, by ship length and leg distance, February 2019.

Figure 6 and Figure 7 also show the consistent trend of electrification potential within each trip length and ship size category. For passenger ferries shown in Figure 6, to achieve a target of at least 50% fossil fuel replacement, electrification needs to target ships up to the size of 55 m on average and routes up to 100 km. For ro-pax ferries shown in Figure 7, the same target is more difficult to attain, as ships up to 170 m in length and routes up to 200 km in distance need to be electrified.

Discussion

In February 2019, ferry operations in China's coastal waters consumed roughly 15,000 tonnes of fossil fuel. A total of 129 passenger ferries and 80 ro-pax ferries completed more than 16,000 legs, more than two-thirds of which took place in the Pearl River Delta region. This working paper explores the potential for Chinese coastal ferries to use battery-electric technology instead of fossil fuels.

Without changing the design of a ship, we hypothetically replaced the existing ship's propulsion and fuel supply system with a battery system to evaluate whether such systems can fulfill the ferries' existing transportation services. We found that the battery range of a ship is limited by a ship's available mass capacity, because a mass-based range is usually shorter than a volume-based range. We found that more than 90% of ferries studied demonstrate theoretical battery ranges long enough to span most legs assigned to them. Even though this result is based on near-future battery technology assumptions (energy density: 370 kWh/m³; specific energy: 200 kWh/tonne), current battery technology assumptions (energy density: 72 kWh/m³; specific energy: 75 kWh/tonne) would be suitable for achieving most legs, especially on smaller ferries. Battery technology improvements only play a key role in the harder-to-electrify segment of existing ferry operations, namely larger ro-pax ferries deployed on longer routes.

The actual feasibility of electrifying ferry operations is limited by charging constraints, ship size, and leg distance. Charging power limits how much energy can be taken onboard the ship while it is waiting at berth. Larger ships require more energy and take longer to recharge. Without charging constraints, medium-sized ships are the easiest to electrify, which is consistent with our findings in earlier work that found medium-sized container ships were most suited for using hydrogen powered fuel cells (Mao et al., 2020). Regarding leg distance, longer legs were more difficult to electrify. We assumed that ships would continue to follow their existing operational schedules in the future, meaning traveling at the same speeds and spending the same amount of time at berth as they currently do. Operations could be adjusted to make it easier to electrify ferries, such as the deployment of additional ships in order to allow more time at berth for recharging while maintaining the same level of transportation services.

In this study, we were mostly interested in charging constraints presented by charging power, as this is where technological improvement could play an important role. In the early stages of e-ferry deployment, charging station designs are more likely to be customized to fit local grid capacity, land availability for onshore battery storage, receiving ship design, and cost. Currently, the *MS Ampere* e-ferry is served with an integrated docking-and-charging system called FerryCHARGER with an effective charging power between 0.8 and 1.2 MW (Martinsen, Elsebutangen, & Solberg, 2019). The *Ellen* e-ferry is served with onshore charging stations with a charging power as high as 4 MW. There has been steady research progress in inductive wireless charging to allow for high-power fast charging. In general, a power transfer capability of approximately 500 kW/m² has been found to be reasonable with the available materials and cooling requirements of the coils

(Guidi, Suul, Jensen, & Sorfonn, 2017). Such a system has been demonstrated in a hybrid plug-in ferry, the *MS Folgefonn*, which has shown a power transfer level exceeding 1 MW. With this type of charging, it would require a 20 m² charging pad installed on one side of the ship to deliver a charging power equivalent to 10 MW, which is not unreasonably large compared to a medium-size ferry.

Conclusions and future work

This study analyzed the operational profiles of Chinese coastal ferries, their energy demand, and the implied battery system to evaluate the feasibility of repowering the fleet with battery-electric technology and discussed regions and market segments where the transition to battery-electric ferries might take off first.

We found that current battery technologies can already satisfy most application scenarios for China's coastal fleet, namely smaller ferries deployed on shorter routes, which could be the first movers of battery-electric ship uptake. Most ferry legs in coastal China are shorter than 200 km, which is well within the battery range values of most ferries studied. Battery technology improvements would help electrify other more difficult segments of the existing ferry operations, namely larger ro-pax ferries deployed on longer routes. In addition, higher charging power during at-berth time helps improve the continuity of ferry operations using batteries, which is crucial for application scenarios where one route is exclusively served by one ship.

If policymakers wish to prioritize better electric ferry deployment, they may wish to focus first on electrifying smaller ships and shorter legs. We found electrifying passenger ferries up to 55 m that sail on legs up to 100 km would replace 50% of fossil fuel use with electricity. For ro-pax ferries, the same fossil fuel replacement target can be attained by targeting ships up to 170 m in length traveling on legs up to 200 km. Among the more than 16,000 legs sailed in February 2019, more than two-thirds took place in the Pearl River Delta region. Electrifying all coastal ferry operations in this region could eliminate more than 30% of the fossil fuel that was used by the entire Chinese coastal ferry fleet in February 2019. Electrifying ferry operations in the Bo Sea region and the Hainan Strait, where substantial ferry activity occurs, could enable additional fossil fuel replacement of more than 40%.

The methods developed in this paper can be applied to other regions and to other ship types. Future work could estimate the costs of electrifying the Chinese coastal ferry fleet and this work could be expanded to cover inland ferries. Future work should also estimate the well-to-wake carbon dioxide equivalent (CO₂e) emissions of battery electric ferries to understand lifecycle CO₂e reduction potential and associated benefits of policies that encourage or require ferry electrification. China's grid life-cycle carbon emission factor is projected to be 635 grams of CO₂e per kWh (100-year global warming potential) in 2020,⁸ which is far from zero or low carbon. However, China has pledged to peak CO₂ emissions by 2030 and endeavors to reach carbon neutrality by 2060 (Myers, 2020). We anticipate that the grid will become less carbon intensive over time, so that an e-ferry fleet would deliver substantial life-cycle CO₂e reductions.

8 This is stated as a goal in China's 13th Five-Year-Plan for the power sector, available in Chinese at <http://www.gov.cn/xinwen/2016-12/22/5151549/files/696e98c57ecd49c289968ae2d77ed583.pdf>

References

- An, K., & Lo, H. K. (2014). Ferry service network design with stochastic demand under user equilibrium flows. *Transportation Research Part B: Methodological*, 66, 70–89. <https://doi.org/10.1016/j.trb.2013.10.008>
- Andersen, J., Crainic, T. G., & Christiansen, M. (2009). Service network design with management and coordination of multiple fleets. *European Journal of Operational Research*, 193(2), 377–389. <https://doi.org/10.1016/j.ejor.2007.10.057>
- Argonne National Lab (2020). *BatPaC model software*. Argonne National Laboratory. <https://www.anl.gov/cse/batpac-model-software>
- Cao, X., & Ye, F. (2020, June 24). All-electric ferry “JUN LV HAO” made its maiden voyage in Wuhan. *Changjiang Daily*. http://m.xinhuanet.com/hb/2020-06/24/c_1126152950.htm
- Cheemakurthy, H., Tanko, M., & Garme, K. (2018). *Urban waterborne public transport systems: An overview of existing operations in world cities*. <https://doi.org/10.13140/RG.2.2.32606.69446>
- Chinese all-electric river cruise vessel is set to break records. (2021, January 10). *The Maritime Executive*. Retrieved from <https://www.maritime-executive.com/article/chinese-all-electric-river-cruise-vessel-is-set-to-break-record>
- Chu, X., Shao, S., Xu, S. X., & Kang, K. (2020). Data-driven ferry network design with candidate service arcs: The case of Zhuhai Islands in China. *Maritime Policy & Management*, 47(5), 598–614. <https://doi.org/10.1080/03088839.2020.1747650>
- Comer, B. (2019). *Transitioning away from heavy fuel oil in Arctic shipping*. Retrieved from the International Council on Clean Transportation, <https://theicct.org/publications/transitioning-away-heavy-fuel-oil-arctic-shipping>
- Faber, J., Hanayama, S., Zhang, S., Pereda, P., Comer, B., Hauerhof, E., ... Xing, H. (2020). *Fourth IMO greenhouse gas study 2020 executive summary*. International Maritime Organization. Retrieved from <https://wwwcdn.imo.org/localresources/en/OurWork/Environment/Documents/Fourth%20IMO%20GHG%20Study%202020%20Executive-Summary.pdf>
- Georgeff, E., Mao, X., Rutherford, D., & Osipova, L. (2020). *Liquid hydrogen refueling infrastructure to support a zero-emission U.S.–China container shipping corridor*. Retrieved from the International Council on Clean Transportation <https://theicct.org/publications/ZEV-port-infrastructure-hydrogen-2020>
- Graser, A. (2019). MovingPandas: Efficient structures for movement data in Python. *GI_Forum*, 7(1), 54–68. https://doi.org/10.1553/giscience2019_01_s54
- Graver, B., Rutherford, D., & Zheng, S. (2020). *CO2 emissions from commercial aviation: 2013, 2018, and 2019*. Retrieved from the International Council on Clean Transportation, <https://theicct.org/publications/co2-emissions-commercial-aviation-2020>
- Guidi, G., Suul, J. A., Jensen, F., & Sorfonn, I. (2017). Wireless charging for ships: High-power inductive charging for battery electric and plug-in hybrid vessels. *IEEE Electrification Magazine*, 5(3), 22–32. <https://doi.org/10.1109/MELE.2017.2718829>
- Hall, D., Pavlenko, N., & Lutsey, N. (2018). *Beyond road vehicles: Survey of zero-emission technology options across the transport sector*. Retrieved from the International Council on Clean Transportation, <https://theicct.org/publications/zero-emission-beyond-road-vehicles>
- Kristensen, J., Nielsen, C. B., & Heinemann, T. (2018). The E-ferry: Energy efficient hull design. *Proceedings of 7th Transport Research Arena TRA 2018*, Vienna, Austria. Retrieved from https://www.el-færgeprojekt.dk/Admin/Public/DWSDownload.aspx?File=%2Ffiles%2Ffiles%2Felf%2C3%A6rge%2Fportal_kristensen%2520et%2520al_2018_tra.pdf
- Lai, M. F., & Lo, H. K. (2004). Ferry service network design: Optimal fleet size, routing, and scheduling. *Transportation Research Part A: Policy and Practice*, 38(4), 305–328. <https://doi.org/10.1016/j.tra.2003.08.003>
- Leung, A., Tanko, M., Burke, M., & Shui, C. S. (2017). Bridges, tunnels, and ferries: Connectivity, transport, and the future of Hong Kong’s outlying islands. *Island Studies Journal*, 12(2), 61–82. <https://doi.org/10.24043/isj.24>

- Mao, X., Rutherford, D., Osipova, L., & Comer, B. (2020). *Refueling assessment of a zero-emission container corridor between China and the United States: Could hydrogen replace fossil fuels?* Retrieved from the International Council on Clean Transportation, <https://theicct.org/publications/zero-emission-container-corridor-hydrogen-2020>
- Martinsen, T., Elsebutangen, H., & Solberg, H. (2019). *Multi-service charging station and/ or onshore energy storage at port for electric ferry-A case study from Norway*. AIM. <https://doi.org/10.34890/702>
- Ministry of Transport of People's Republic of China. (2020a). *2019 statistical bulletin of transport industry development*. Retrieved February 19, 2021, from http://xxgk.mot.gov.cn/2020/jigou/zghs/202006/t20200630_3321335.html
- Ministry of Transport of People's Republic of China. (2020b). *Guidelines for developing inland waterborne transport*. Retrieved February 19, 2021, from http://xxgk.mot.gov.cn/2020/jigou/zghs/202006/t20200630_3321348.html
- Minnehan, J. J., & Pratt, J. W. (2017). *Practical application limits of fuel cells and batteries for zero emission vessels*. Retrieved from <https://doi.org/10.2172/1410178>
- Myers, S. L. (2020, September 23). China's pledge to be carbon neutral by 2060: What it means. *The New York Times*. Retrieved from <https://www.nytimes.com/2020/09/23/world/asia/china-climate-change.html>
- National Geospatial-Intelligence Agency. (2019). *World Port Index* (Pub. 150). Retrieved from <https://msi.nga.mil/Publications/WPI>
- Olmer, N., Comer, B., Roy, B., Mao, X., & Rutherford, D. (2017). *Greenhouse gas emissions from global shipping, 2013-2015*. Retrieved from the International Council on Clean Transportation, <https://theicct.org/publications/GHG-emissions-global-shipping-2013-2015>
- Slowik, P., Lutsey, N., & Hsu, C. (2020) *How technology, recycling, and policy can mitigate supply risks to the long-term transition to zero-emission vehicles*. Retrieved from the International Council on Clean Transportation, <https://theicct.org/publications/mitigating-zev-supply-risks-dec2020>
- Wang, D. Z. W., & Lo, H. K. (2008). Multi-fleet ferry service network design with passenger preferences for differential services. *Transportation Research Part B: Methodological*, 42(9), 798-822. <https://doi.org/10.1016/j.trb.2008.01.008>